

Vortex Pinball Under Crossed AC Drives in Superconductors with Periodic Pinning Arrays

C. Reichhardt and C.J. Olson

Center for Nonlinear Studies and Applied Theoretical and Computational Physics Division, Los Alamos National Laboratory, Los Alamos, NM 87545

(October 27, 2018)

Vortices driven with both a transverse and a longitudinal AC drive which are out of phase are shown to exhibit a novel commensuration-incommensuration effect when interacting with periodic substrates. For different AC driving parameters, the motion of the vortices forms commensurate orbits with the periodicity of the pinning array. When the commensurate orbits are present, there is a finite DC critical depinning threshold, while for the incommensurate phases the vortices are delocalized and the DC depinning threshold is absent.

PACS numbers: 74.60.Ge,74.60.Jg

A wide variety of dynamical systems can be modeled as a classical particle moving in a periodic potential. Examples of such systems are Josephson-junction (JJ) arrays [1,2], sliding charge density waves (CDW) [3,4], atomic friction [5], vortices in superconductors moving over periodic substrates [6–12], electrons at low magnetic fields in antidot arrays [13,14], as well as ions [15] and colloids [16] in optical trap arrays. When an AC drive is superimposed over the DC drive, resonances or phase-locking effects can occur which have been extensively studied in JJ arrays [2] and CDWs [3]. Signatures of the phase locking include oscillations in the depinning threshold with increasing AC drive amplitude, and locking of the particle velocity to a fixed value over a range of the DC drive. In superconductors with periodic substrates, phase locking of driven vortices has been experimentally observed in samples containing 1D periodic modulations [6]. More recently, experiments, simulations, and theory have shown that in superconductors with periodic hole arrays, phase locking or Shapiro steps occur when combined DC and AC drives are applied.

In all these phase locking systems the AC and DC drives are in the *same direction* and the motion can be considered effectively one-dimensional (1D). Different effects can arise in a two-dimensional (2D) system. Recently it was shown that new kinds of phase-locking effects occur when the AC drive is applied *perpendicular* to the DC drive for systems with periodic substrates [12].

Here we study vortex motion in superconductors with periodic arrays of pinning sites and *three* combined driving forces. A DC drive f_{dc} is applied along the longitudinal direction, and *two* AC drives which are 90 degrees out of phase are added in the longitudinal and transverse directions. In the absence of pinning and at $f_{dc} = 0$, the vortices move in a circular orbit with radius and eccentricity determined by the amplitudes and frequencies of the AC drives. We focus on a regime just above the first matching field B_ϕ , where each pin is occupied by one vortex and a small number of additional vortices move in the periodic potential created by the pinned vortices. The existence of such interstitial vortices above B_ϕ has been

inferred from transport measurements and direct imaging in samples with periodic holes [7], and in this same regime Shapiro steps have previously been observed [9].

The system we propose has similarities to the “electron pinball” model studied by Weiss *et al.* [13] and others [14], in which classical cyclotron electron motion is induced by a magnetic field in samples with periodic arrays of antidots. In these systems, peaks and dips appear in the magnetoresistance as a function of field. The features are believed to arise when classically moving electrons follow *pinned* or *commensurate* circular orbits enclosing integer numbers of dots, in which the electrons can travel without scattering off the dot potentials. At the *incommensurate* orbits the electrons are scattered and diffuse throughout the sample. There are important differences between the vortex “pinball” system and the electron systems. The vortices interact with a *long-range* smooth or egg-carton square potential, rather than simple point scatters, and thus the moving vortices must follow square orbits (in the case of square pinning arrays), rather than circular orbits. A particularly attractive feature of the vortex system is that the *shape* of the orbit can be carefully controlled experimentally by changing the ratio of the AC amplitudes, phases or frequencies. This allows new kinds of anisotropic orbits and commensuration effects to be produced, which are not obtainable in the electron pinball models.

We consider a thin superconductor containing 2D vortices, which is the appropriate model for the recent experiments in superconductors with hole and dot arrays. The vortex-vortex interaction has the form of a logarithmic potential, $U_v = -A_v \ln(r)$, with the energy normalization $A_v = \Phi_0^2/8\pi\Lambda$. Here, Φ_0 is the flux quantum and Λ is the effective 2D penetration depth for a thin film superconductor. The overdamped normalized equation of motion for a single vortex i is

$$\mathbf{f}_i = \eta \frac{d\mathbf{r}_i}{dt} = \mathbf{f}_i^{vv} + \mathbf{f}_i^{vp} + \mathbf{f}_{dc} + \mathbf{f}_{ac} = \eta \mathbf{v}_i \quad (1)$$

where the damping term η is the Bardeen-Stephen friction. The force from vortex i on the other vortices is

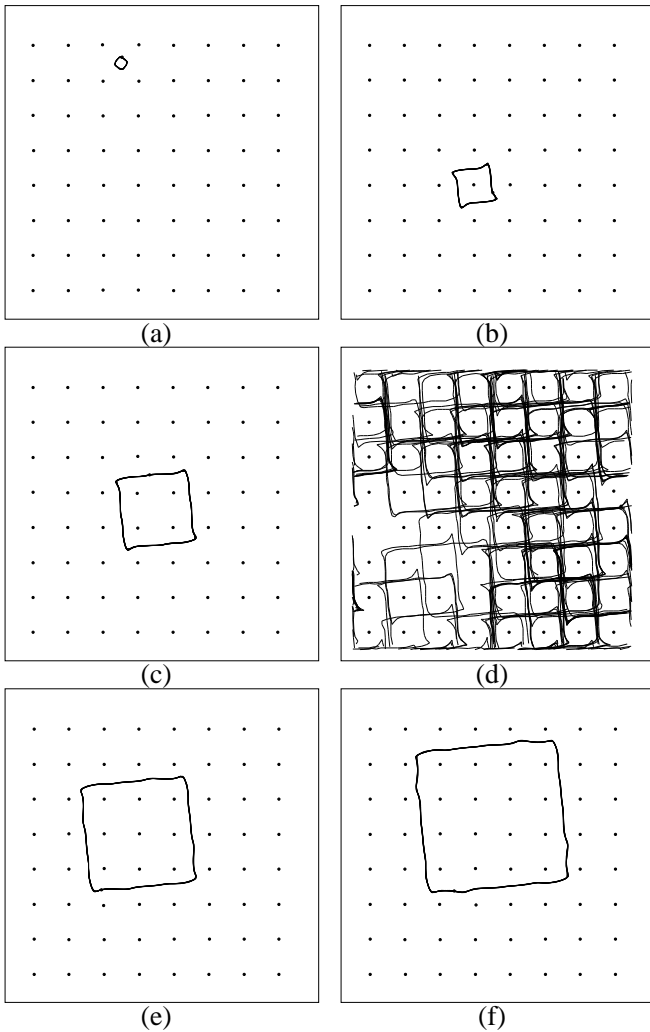


FIG. 1. Vortex positions (dots) and trajectories (lines) for $f_{dc} = 0.0$ and different isotropic AC amplitudes. (a) $A = 0.16$, (b) $A = 0.21$, (c) $A = 0.3$, (d) $A = 0.355$, (e) $A = 0.39$, and (f) $A = 0.47$.

$\mathbf{f}_i^{vv} = -\sum_{j \neq i}^{N_v} \nabla_i U_v(r_{ij})$. The long range interaction is treated with a fast converging summation method [17]. The pinning force \mathbf{f}^{vp} arises from the pinning sites which are modeled as short range attractive parabolic wells. The pinning sites are placed in a square array of side L , and each pin has a radius of $r_p = 0.15L$, which is within the typical experimental ratios of $r_p/L = 0.14$ to 0.3 . The DC driving term \mathbf{f}_{dc} is applied along the symmetry axis of the pinning array, in the x -direction. The AC driving term is $\mathbf{f}_{AC} = A \sin(\omega_A t) \hat{\mathbf{x}} + B \cos(\omega_B t) \hat{\mathbf{y}}$, where we fix $w_A/w_B = 1.0$. For most of the results presented here we consider the case of a system containing 64 pins and a vortex filling fraction of $B/B_\phi = 1 + 1/64$; however, we have found the same results for higher filling fractions (such as $B/B_\phi = 2, 7/4, 3/2$, and $5/4$) at which the interstitial vortices form a symmetric pattern so that interstitial vortex interactions cancel. The initial vortex position is found by annealing from a high temperature

with no driving and cooling to $T = 0$. The DC drive is increased in increments of 0.0001 and the sample is held at each drive for 3×10^5 time steps to ensure a steady state; the DC depinning threshold is determined from the time averaged vortex velocities $\langle V_x \rangle$.

We first consider the case of isotropic AC driving with $A/B = 1.0$ and show that commensurate-incommensurate depinning transitions occur as a function of increasing A even at $f_{dc} = 0$. Example vortex trajectories are illustrated in Fig. 1. For $A = 0.16$ [Fig. 1(a)] the vortex is confined to move in a small circular orbit in the middle of the plaquette. For $A = 0.21$ [Fig. 1(b)] the AC amplitude is large enough that the vortex encircles $n = 1$ pin in an orbit that is slightly tilted due to the counter-clockwise vortex movement through the square potential. In Fig. 1(c), for $A = 0.3$, the orbit encircles $n = 4$ pins. In Fig. 1(d), for $A = 0.355$, the orbit radius is somewhere between $n = 4$ and $n = 9$, and the vortex interacts strongly with the occupied pins, scattering off them. The vortex becomes delocalized, and diffuses throughout the sample, avoiding areas near pins due to the repulsion from the pinned vortices. The orbit switches intermittently between $n = 4$ and $n = 9$. In Fig. 1(e,f) we show localized vortex orbits for $A = 0.39$ and 0.47 , with $n = 9$ and $n = 16$, respectively. We also find a stable orbit with $n = 25$ for $A = 0.57$. For $0.42 < A < 0.45$, as well as for $0.52 < A < 0.55$, the vortex is delocalized and moves in a manner similar to that shown in Fig. 1(d).

In general we find localized orbits at values of A for which the vortex trajectory encloses $n = m^2$ pins, where m is an integer. By comparison, in electrons in antidot lattices, Weiss *et al.* [13] found commensurate or pinned orbits when the number of dots encircled was $n = 1, 2, 4, 9, 16$, and 21 . We do not observe any stable orbits for $n = 2$ and 21 . In the electron systems [13,14] these orbits correspond to states where a portion of the electron orbit closely approaches the dots, which are point scatterers. In the vortex system, due to the long range vortex-vortex interactions, the mobile vortices cannot follow orbits that approach arbitrarily closely to the pinning sites.

In Fig. 2 we show the DC depinning threshold F_{dp}/F_{dp}^0 vs A for the isotropic case $A = B$. Here, F_{dp}^0 is the DC depinning force for $A = 0$. The commensurate orbits are *pinned* at low f_{dc} , producing a series of peaks in F_{dp} at the commensurate AC values. At the incommensurate phases the depinning threshold vanishes. For $0.0 < A < 0.2$, the vortices move in the $n = 0$ interstitial orbit illustrated in Fig. 1(a). F_{dc} decreases as the AC amplitude increases until reaching a minimum value at $A = 0.19$, followed by a peak in F_{dc} for $A = 0.225$, which corresponds to an $n = 1$ orbit [Fig. 1(b)]. The second peak at $A = 0.31$ corresponds to the $n = 4$ orbit [Fig. 1(c)]. For the delocalized incommensurate orbits [Fig. 1(d)] of $0.34 < A < 0.36$, F_{dp} vanishes. A finite F_{dp}

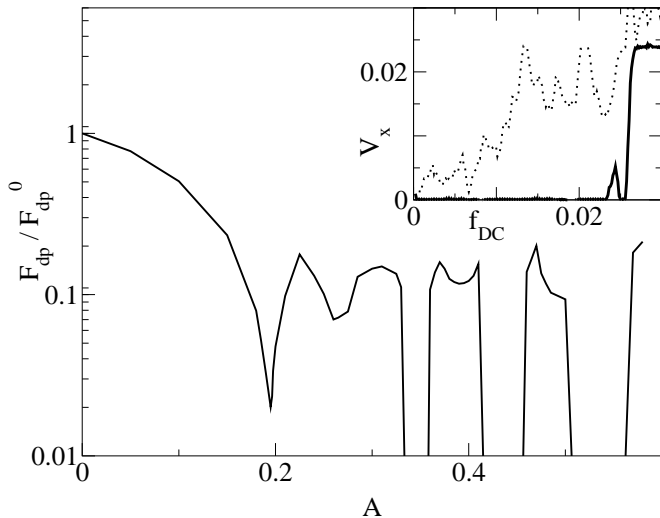


FIG. 2. The DC depinning force F_{dp}/F_{dp}^0 vs AC amplitude A for the isotropic case $A = B$. F_{dp}^0 is the depinning force for zero AC drive. Inset: average DC velocity $\langle V_x \rangle$ vs DC driving force f_{dc} for an incommensurate orbit $A = 0.43$ (dotted line) and a commensurate orbit $A = 0.37$ (solid line).

is regained when $n = 9$ orbits appear for $0.36 < A < 0.42$. As A continues to increase, F_{dp} is nonzero for A values at which the stable $n = 16$ and $n = 25$ orbits are observed, with $F_{dp} = 0$ in portions of the regions between these values of A . We have checked the oscillatory behavior for different values of L and find the same general behavior. Since the radius of the vortex orbit $R \sim A/\omega_A$, a similar series of peaks in F_{dc} occurs if A is fixed and $1/\omega_A$ is varied. In the inset of Fig. 2 we show typical curves of the average DC velocity $\langle V_x \rangle$ vs f_{dc} for an unpinned incommensurate orbit at $A = 0.43$ and a pinned commensurate orbit at $A = 0.37$, illustrating the well defined sharp depinning threshold for the pinned orbits.

The maximum F_{dp} values in Fig. 2 do *not* decrease with increasing A , indicating that all of the commensurate orbits are pinned equally well. In addition the boundaries between the pinned and unpinned regions are sharp. Thus the behavior of F_{dp} vs A clearly differs from that associated with Shapiro steps [1,2,10], where the depinning threshold oscillates with A according to a Bessel function $J_0(A)$, the peaks in the depinning force are smooth, and the peak F_{dp} value gradually decreases with A .

We next consider anisotropic or elliptical orbits for $A \neq B$. In Fig. 3 we show F_{dp}/F_{dp}^* vs B/A for fixed $A = 0.225$ and varying B , where F_{dp}^* is the depinning force for $B = 0$. Again we find strongly pinned orbits, indicated by peaks in F_{dp} ; however, in this case the pinned orbits occur when the vortex orbit encircles $n = m$ pins. If a higher value of A is chosen such that the orbit encircles two pinning sites in the transverse direction in one period, commensurate orbits that encircle $n = 2m$ pins appear. The peaks in the depinning curve shown here are much more symmetric than those in Fig. 2. This may be due

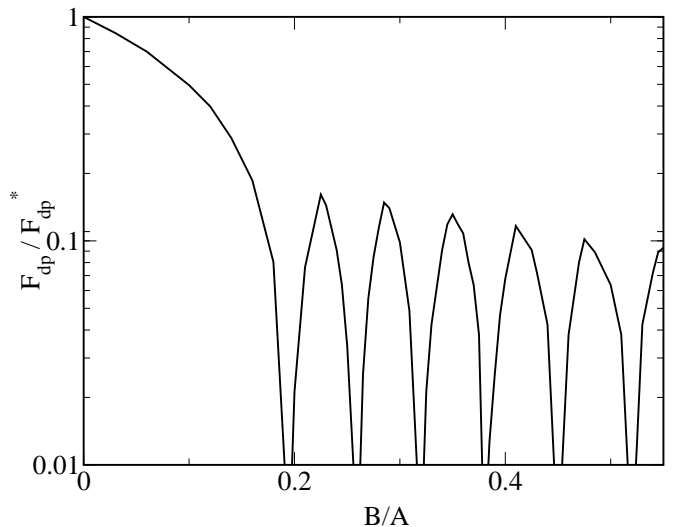


FIG. 3. The DC depinning force F_{dp}/F_{dp}^* vs AC amplitude B/A for the anisotropic case where $A = 0.225$ and B is varied. F_{dp}^* is the depinning force for $B = 0.0$.

to the fact that the elliptical orbits are less perturbed by the square pinning potential than the isotropic circular orbits.

In Fig. 4 we present several anisotropic commensurate orbits at the depinning peaks shown in Fig. 3. Here the orbits for Fig. 4(a,b,d) encircle $n = 1, 2,$ and 3 pins, respectively. This trend continues for the higher peaks. In Fig. 4(c) we also show a *sliding* orbit at $B = 0.3$ with f_{dc} above depinning.

We now discuss experimental systems in which these phases can be observed. For superconductors with periodic antidot arrays, the pin geometry should be chosen such that the pins have vortex saturation numbers of one, so that above B_ϕ the additional vortices will sit in the interstitial regions. For pins with higher saturation numbers, commensuration effects should still be observable at higher matching fields when interstitial vortices start to appear. Samples with very low intrinsic pinning should be used to enhance the effect. Samples in which Shapiro steps for moving interstitial vortices have been observed would be ideal. As in the case of Shapiro steps [10], the variation of the depinning force versus AC drive amplitude should be most pronounced at filling fractions where the interstitial vortices form a symmetrical pattern and the interstitial vortex interactions effectively cancel, such as at $B/B_\phi = 2.0, 1.75, 1.5,$ and 1.25 . Using samples such those in Ref. [9] where Shapiro steps are observed, for a pinning lattice spacing of $a = 2\mu m$, $\omega = 2\pi\nu$, and $\nu = 40 MHz$, commensuration effects should be observable with applied crossed AC currents from 0 to $10 I_c$ where I_c is the critical current. Superconductors with rectangular and triangular (rather than square) pinning arrays should also exhibit these phenomena; however, the stable orbits would encircle different numbers of pins than the orbits described here. In superconductors with

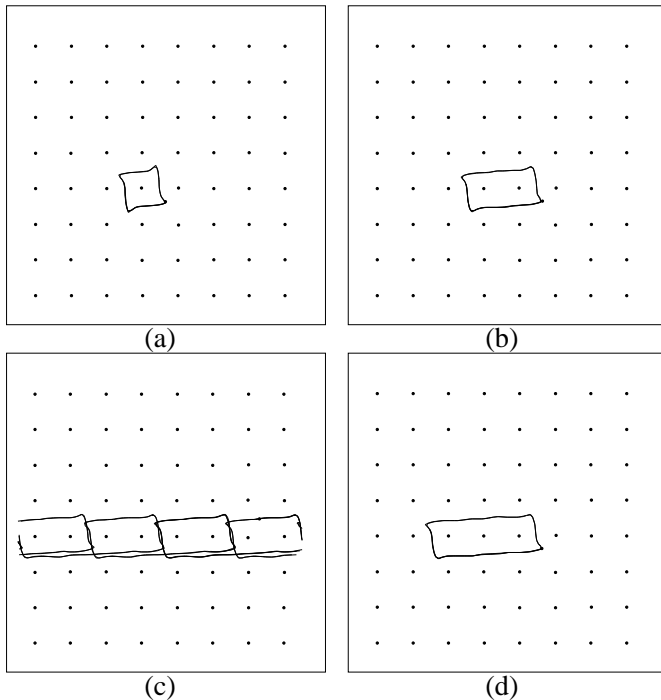


FIG. 4. Vortex positions (dots) and trajectories (lines) for fixed $A = 0.225$ and (a) $B = 0.225$, (b) $B = 0.285$ and (d) $B = 0.35$. In (c) a sliding orbit is shown for $B = 0.3$ and $f_{ac} > F_{dp}$.

magnetic dot arrays, the dots can act as long range repulsive sites, so that pinned orbits of the type described here could be observed at vortex filling fractions such as $B/B_\phi = 1$ and $1/2$. In addition, superconductors with 2D smoothly modulated surfaces should also produce commensurate and incommensurate orbits. Other promising systems in which these phases could be observed include 2D JJ arrays, 2D atomic friction models, and colloids on optical pin-scapes [16]. A possible application of our results would be particle segregation in multi-species systems, such as colloids on periodic substrates, where the different species have different mobilities. Here it should be possible to tune the AC drive such that one species would be pinned and another depinned. The species could then be segregated with a DC drive.

To summarize, we have numerically studied the motion of vortices interacting with a 2D periodic potential created by immobile vortices located at pinning sites placed in a square array. We apply *two* AC drives, perpendicular to one another and out of phase by 90° , such that the vortices move in a circle in the absence of a substrate potential. For AC drives of equal amplitude, as a function of increasing AC amplitude we find a series of pinned orbits enclosing $n = m^2$ pinning sites. Each of these orbits has a finite depinning threshold to an additional applied DC force. At AC amplitude values between these pinned orbits, the vortices are delocalized and diffuse through the sample, and the DC depinning threshold is zero. Experimentally these states can be observed as a series of

pinned and non-pinned regions as a function of AC amplitude or frequency. For anisotropic AC drives, we find a series of asymmetric pinned orbits which enclose $n = m$ pinning sites. We call our model the vortex pinball model in analogy to the electron pinball system for electron cyclotron motion in anti-dot arrays. We also suggest other systems in which these phases can be observed experimentally.

Acknowledgements: This work was supported by the US Dept. of Energy under contract W-7405-ENG-36.

-
- [1] A. Barone and G. Paterno, *Physics and Applications of the Josephson Effect* (Wiley, New York, 1982).
 - [2] S.P. Benz *et al.*, Phys. Rev. Lett. **64**, 693 (1990); K.H. Lee, D. Stroud and J.S. Chung, Phys. Rev. Lett. **64**, 692 (1990); M. Octavio *et al.*, Phys. Rev. B **44**, 4601 (1991); D. Dominguez and J.V. Jose, Phys. Rev. Lett. **69**, 514 (1992).
 - [3] G. Gruner, Rev. Mod. Phys. **60**, 1129 (1988); R.E. Thorne, Physics Today **49**, no. 5, 42 (1996).
 - [4] R.E. Thorne *et al.*, Phys. Rev. B **35**, 6360 (1987); M.J. Higgins, A.A. Middleton, and S. Bhattacharya, Phys. Rev. Lett. **70**, 3784 (1993).
 - [5] B.N.J. Persson, *Sliding Friction: Physical Principles and Applications* (Springer, Heidelberg, 1998); E. Granato and S.C. Ying, Phys. Rev. Lett. **85**, 5368 (2000); O.M. Braun *et al.*, Phys. Rev. E. **63**, 036129 (2001).
 - [6] P. Martinoli *et al.*, Sol. St. Commun. **17**, 205 (1975).
 - [7] A.T. Fiory, A.F. Hebard, and S. Somekh, Appl. Phys. Lett. **32**, 73 (1978); M. Baert *et al.*, Phys. Rev. Lett. **74**, 3269 (1995); K. Harada *et al.*, Science **274**, 1167 (1996); V.V. Metlushko *et al.*, Phys. Rev. B **59**, 603 (1999).
 - [8] C. Reichhardt, C.J. Olson and F. Nori, Phys. Rev. Lett. **78**, 2648 (1997); C. Reichhardt and F. Nori, Phys. Rev. Lett. **82**, 414 (1999); V.I. Marconi and D. Dominguez, Phys. Rev. Lett. **82**, 4922 (1999); G. Carneiro, Phys. Rev. B **62**, R14661 (2000); V. Gotcheva and S. Teitel, Phys. Rev. Lett. **86**, 2126 (2001).
 - [9] L. Van Look *et al.*, Phys. Rev. B **60**, R6998 (1999).
 - [10] C. Reichhardt *et al.*, Phys. Rev. B **61**, R11 914 (2000).
 - [11] J.I. Martin *et al.*, Phys. Rev. Lett. **79**, 1927 (1997); D.J. Morgan and J.B. Ketterson, Phys. Rev. Lett. **80**, 3514 (1998); J.I. Martin *et al.*, Phys. Rev. Lett. **83**, 1022 (1999); M.J. van Bael *et al.*, Phys. Rev. Lett. **86**, 155 (2001).
 - [12] C. Reichhardt *et al.*, Phys. Rev. B **64**, 134508 (2001).
 - [13] D. Weiss *et al.*, Phys. Rev. Lett. **66**, 2790 (1991).
 - [14] R. Fleischmann, T. Geisel and R. Ketzmerick, Phys. Rev. Lett. **68**, 1367 (1992); J.H. Smet, Phys. Rev. Lett. **80**, 4538 (1998); J. Wiersig and K.H. Ahn, Phys. Rev. Lett. **87**, 6803 (2001).
 - [15] K.I. Petsas *et al.*, Europhys. Lett. **46**, 18 (1999).
 - [16] P. Korda, G.S. Spalding, and D.G. Grier, to be published.
 - [17] N. Grønbech-Jensen, Int. J. Mod. Phys. C **7**, 873 (1996).